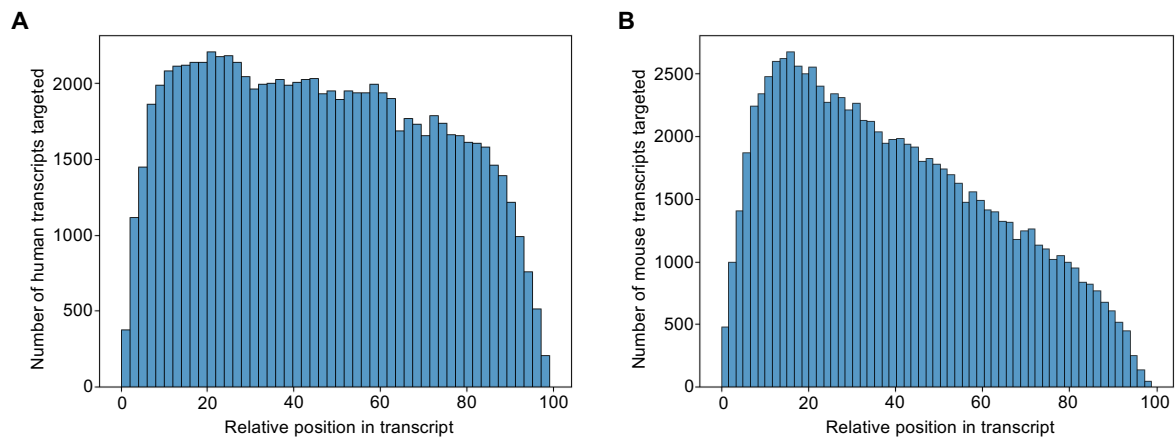
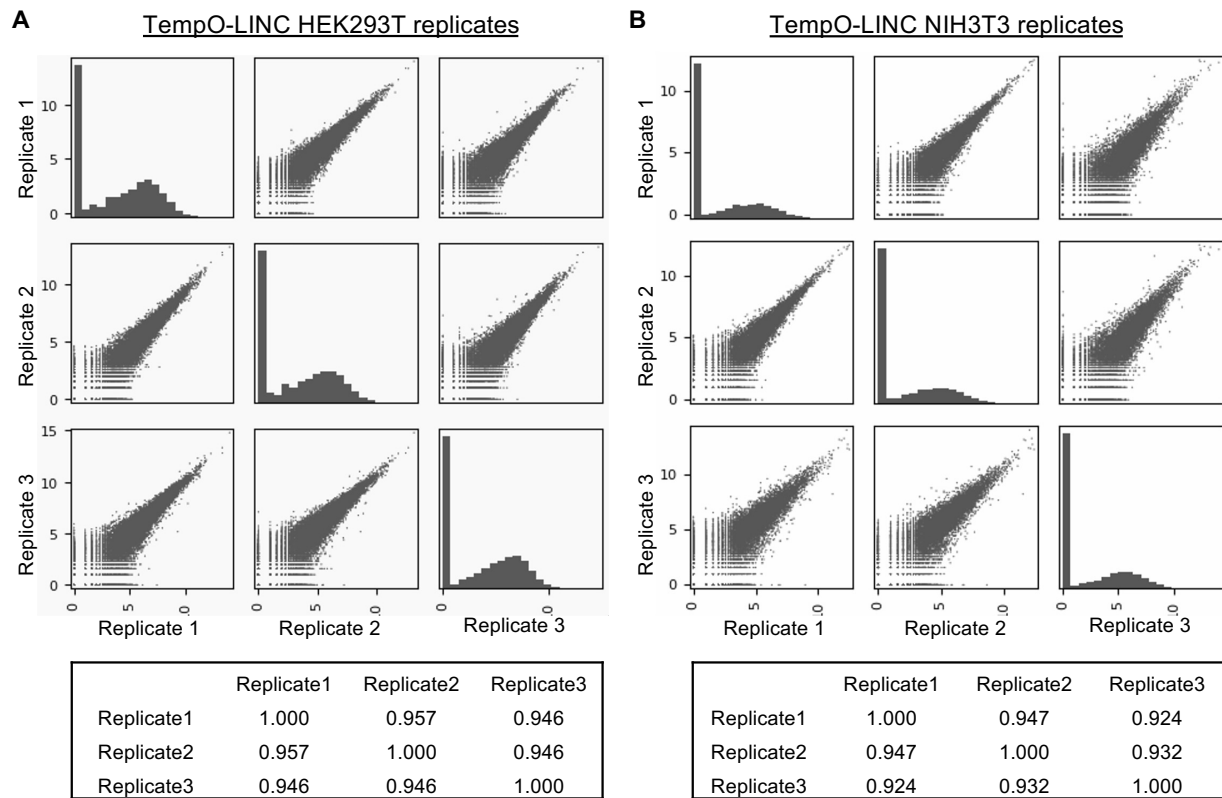


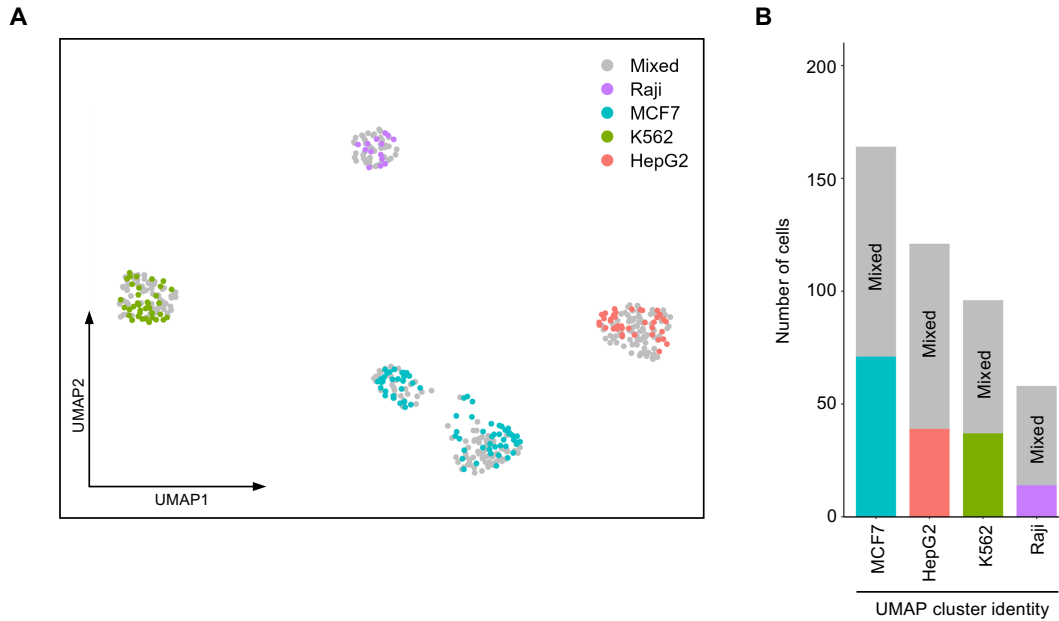
Supplemental Figures



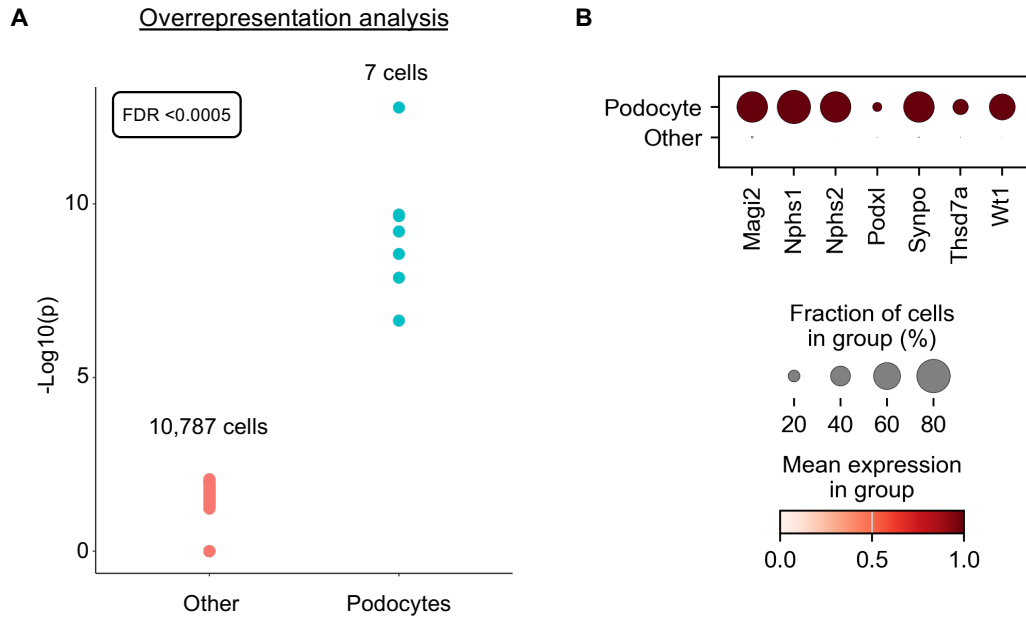
Supplemental Figure 1. Bar plots showing the relative targeting position of DO probes within their target mRNAs with “0” representing the 5’ end and “100” the 3’ end of the message. (A) Analysis of the Human Whole Transcriptome v2.1 (22,533 probe pairs, 19,683 genes) DO pool. (B) Distribution of the Mouse Whole Transcriptome v1.1 (30,146 probe pairs, 21,400 genes) DO pool.



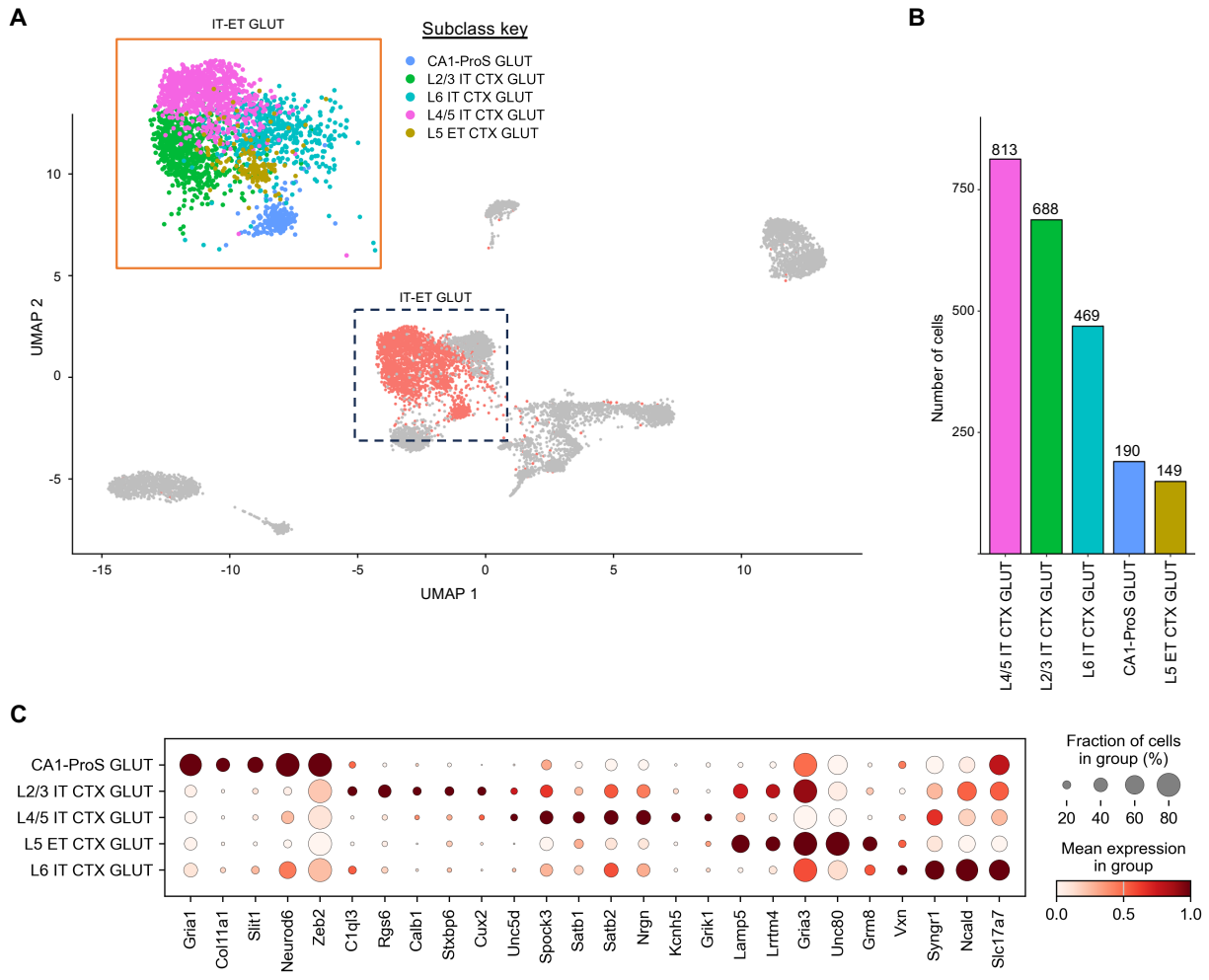
Supplemental Figure 2. (A) The scatterplot matrix shows the correlation between the sum of the log₂ transformed read counts from 50 random human HEK293T cells across three TempO-LINC replicates. Plots reported in the diagonal of the matrix show the distribution of the log₂ transformed read counts for each replicate (x axis = log₂ transformed sum of counts from 50 random cells, y axis: number of genes). Pearson *r* values are reported in the table below the scatterplot matrix. (B) Identical scatterplot matrix shown for the sum of log₂ transformed read counts from 50 random mouse NIH3T3 cells in the three replicates.



Supplemental Figure 3. (A) Human MCF7, Raji, K562 and HepG2 cell lines as well as a mixture of all four cell lines (Mixed) were simultaneously barcoded with Tempo-LINC for single-cell transcriptome profiling. 439 total cells were identified with a UMAP plot showing four distinct populations of cells identified following unsupervised clustering. Based on the Barcode 1 identity, cells for mixed and independent cell line samples were color coded on the UMAP, demonstrating that Tempo-LINC can correctly resolve cell type identity from mixed populations of human cells. (B) Bar plot showing the number of cells associated with each of the 4 major UMAP populations. The number of cells associated with “Mixed” (gray fraction) or cell line-specific barcode sample identities can be seen for each bar on the plot. The precise cell numbers were: 278 total Mixed cells identified and found distributed into all 4 of the cell cluster populations, 71 MCF7 cells, 39 HepG2 cells, 14 Raji cells and 37 K562 cells.



Supplemental Figure 4. Identification of Podocytes from Kidney Tissue. (A) Identification of podocytes within the mouse kidney was performed using overrepresentation analysis utilizing a seven podocyte marker gene set consisting of Nphs1, Nphs2, Podxl, Wt1, Magi2, Synpo and Thsd7a. The false discovery rate (FDR) value was calculated using the Benjamini & Hochberg adjustment method. (B) Dot plot analysis showing expression of seven known molecular markers for podocytes across either the identified podocytes or the 10,787 "other" cells resulting from the overrepresentation analysis in panel "A".



Supplemental Figure 5. Neuronal Subclass Identification within the IT-ET GLUT Cluster. (A) Increasing the cluster resolution on the Seurat generated Figure 4 UMAP demonstrates that 5 additional neuronal cell subclusters can be identified within the IT-ET GLUT population. Dashed box indicates the region on the UMAP in Figure 4 that is magnified in the orange box. IT-ET subclasses identified and annotated include: L2/3 IT CTX GLUT, L4/5 IT CTX GLUT, L6 IT CTX GLUT, L5 ET CTX GLUT and CA1-ProS GLUT. (B) Cell numbers for each subclass are plotted. (C) Dot plot showing expression of 26 subclass specific biomarkers within the 5 identified IT-ET GLUT subclusters.